11

Interaction of Renewable Energy Source and Power Supply Network

Branislav Dobrucký, Michal Pokorný and Mariana Beňová
University of Zilina
Slovak Republic

1. Introduction to interaction of RES and network

Renewable energy systems (RES) become more and more important as the serious sources, first of all from the point of view of improvement of power generating efficiency and effectiveness of operation. RES systems (in this sense) consist of renewable energy source, (e.g. photovoltaics, fuel cells, wind power,..), pre-conditioning unit, DC link, inverter, transformer (if necessary) and inductive coupling with electronic switch or direct connection to power supply network.

The loads and supply system can be operated in three modes of operation: autonomous supply from the network or autonomous supply from RES system, and parallel operation of power supply network and RES(s). The chapter thereinafter deals with parallel operation of the both sources at steady-state and transient dynamic states.

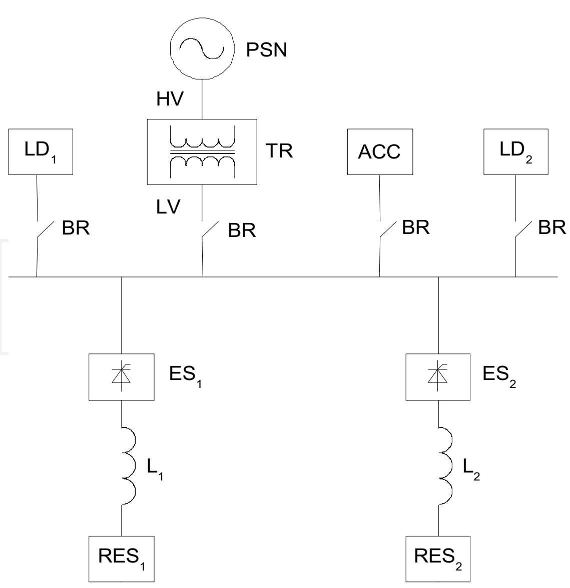

Legend:

PSN – power supply network
HV - high voltage
LV - low voltage
LD - loads
ACC – energy accumulation
BR - breakers
ES - electronic switches
L - separating inductors
RES - renewable energy sources

Fig. 1. Block diagram of power supply network and renewable energy system(s) connection

Interconnection between renewable energy systems RES and power electric network depends on type and power of RES:
- RES with nearly harmonic output voltage, synchronized by grid: direct connection,
- RES with non-harmonic output voltage, synchronized by grid: inductive inter-connection,
- remote RES non-synchronized with grid: HVDC energy transfer.

Single-phase inverters are commonly used to obtain utility grade ac power in small distributed generation systems such as photovoltaics, wind power generators, fuel cells chip systems. When such single-phase systems are aggregated to form microgrids integrable with a three-phase inverter system or a common dc bus, it is desirable to maintain the aggregated power to be constant [Bala & Venkataramanan, 2007]. Various transfigurations of single-phase converter topologies brings [Xue et al, 2004]; [Koutroulis et al, 2001]; [Rajeshekara, 2005]. Large complex wind plants are not explicitly described in this chapter. Their behaviour and back influence on power supply network can be found in [CIGRE, 2007; Spacil, 2006].

The main characteristics of electric power quantities under sinusoidal, non-sinusoidal, balanced, or unbalanced conditions are described in the Standards [IEEE, 1999; IEEE, 2000]. Modelling and simulation of electric power quality parameters differs somewhat from the ordinary power system modelling as far as short -circuit, load flow and transient stability studies are concerned. The reason is that the behaviour of the system equipment must be predicted for frequencies well above the fundamental one [Dumitrescu, 2009; Ghartemani et al, 2004].

All above mentioned problems have to be taken in account during investigation of RES and power network, and proper methods should be used to fulfill the overall goals.

2. Theoretical background for single- and three-phase transients

In general, transient phenomena of RES and power supply network can be investigated by different ways as follows:
- as complex non-linear system, using high volume SW packages (PSCAD/EMTDC, EMTP, EDSA, OrCAD..)
- as linearised system making possible of superposition:
  - in time domain (piece-wise linearization and state-variable method, z-transform and switching function method),
  - in frequency domain (decomposition into single harmonic linear subsystems)

Simulation software packages are a powerful electromagnetic time domain transient simulation environment and study tools. Package usually includes static or dynamic characteristic of the electronic switches, and it works with ***invariant circuit topologic scheme*** and with parametric changes of the system during simulation.

Above mentioned linearisation, superposition method and z-transformation can be conveniently used for investigated electric circuit's analysis.

Piece-wise linearisation in time domain. This method works during simulation with ***periodically variable circuit topologic structure*** of the system, and it uses electronic switches as separators between successive time intervals of operation of the system. Within a single time intervals of operation the topologic structure of the system is to be foreseen as constant one. Therefore one can use state variable method to describe RES system [Mohan et al, 2003; Dobrucky at al, 2007]:

$$\frac{\mathrm{d}}{\mathrm{d}t}(\boldsymbol{x}(t)) = \boldsymbol{A}\cdot\boldsymbol{x}(t)+\boldsymbol{B}\cdot\boldsymbol{u}(t) \qquad (1)$$

where: $\boldsymbol{x}(t)$ is the vector of state variables, $\boldsymbol{A}$, $\boldsymbol{B}$ matrices of system elements, $\boldsymbol{u}(t)$ input vector of exciting functions

$$\boldsymbol{y}(t)=\boldsymbol{C}\cdot\boldsymbol{x}(t)+\sum_{i=0}^{r}\left[\boldsymbol{D}\cdot\boldsymbol{u}^{(i)}(t)\right] \qquad (2)$$

where: $\boldsymbol{y}(t)$ is the vector of output variables, $\boldsymbol{C}$, $\boldsymbol{D}$ system matrices, r highest order of derivatives of the input vector (providing the derivatives exist).

In the next time interval the state variables end-values of the previous time-interval will be considerate as the initial values.

Note: Method of fictitious exciting function could be used in case of non-stationary elements of $\boldsymbol{A}$ matrix of the system.

Using Park-Clarke orthogonal transform and subsequent two orthogonal Fourier series. Any m-phase system (symmetrical or non-symmetrical) can be transformed into equivalent 2-phase orthogonal system using Park-Clarke transform. Transform into stationary α, β-coordinate system is exclusively used in power electronics. That transform is defined by transformation equation

$$\boldsymbol{x}^*(t)=\frac{2}{3}\left[\boldsymbol{x}_1(t)+\mathrm{a}\cdot\boldsymbol{x}_2(t)+\mathrm{a}^2\cdot\boldsymbol{x}_3(t)\right] \qquad (3)$$

where $\mathrm{a}=1\cdot\exp\left(\mathrm{j}\frac{2\cdot\pi}{3}\right)$ and real- and imaginary parts of function (3) for symmetrical system are

$$\boldsymbol{x}_\alpha(t)=\frac{1}{3}\left[2\cdot\boldsymbol{x}_1(t)-\boldsymbol{x}_2(t)-\boldsymbol{x}_3(t)\right], \qquad (4)$$

$$\boldsymbol{x}_\beta(t)=\frac{1}{\sqrt{3}}\left[\boldsymbol{x}_2(t)-\boldsymbol{x}_3(t)\right]. \qquad (5)$$

Since $\boldsymbol{x}^*(t)$ is complex time function (= $\boldsymbol{x}_\alpha(t)$ +j$\boldsymbol{x}_\beta(t)$) the time-waveforms of $\boldsymbol{x}_\alpha(t)$ and $\boldsymbol{x}_\beta(t)$ can be expressed by complex Fourier series [Takeuchi, 1973; Bartsch, 1994]

$$x^*(t)\cong\sum_{k=-\infty}^{\infty}x_k\,e^{\mathrm{j}k\omega t}=x_0+\sum_{k=1}^{\infty}\left(x_k\,e^{\mathrm{j}k\omega t}+x_{-k}\,e^{-\mathrm{j}k\omega t}\right) \qquad (6)$$

Properties of orthogonal Fourier series and convergence is described by [Marcokova, 1995; 2009]; and some application of them are given in [Takeuchi, 1973]; [Zaskalicky&Zaskalicka, 2008].

Using z-transform and switching function method. The renewables, as sources of pulse output voltage series, can be described by system of difference equations.

For three-phase system the currents in α-β coordinates are given as

$$i_\alpha(n+1)=\mathrm{f}_{\mathrm{T}/6}\cdot i_\alpha(n)+\mathrm{g}_{\mathrm{T}/6}\cdot u_\alpha(n) \qquad (7)$$

$$i_\beta(n+1)=\mathrm{f}_{\mathrm{T}/6}\cdot i_\beta(n)+\mathrm{g}_{\mathrm{T}/6}\cdot u_\beta(n) \qquad (8)$$

where $u(n)$ are the voltages in α and β coordinates, respectively

$$u_\alpha(n) = \frac{2}{3} \cdot \sin\left(\frac{n \cdot \pi}{3} + \frac{\pi}{6}\right) \cdot U \tag{9}$$

and

$$u_\beta(n) = \frac{-2}{3} \cdot \cos\left(\frac{n \cdot \pi}{3} + \frac{\pi}{6}\right) \cdot U \tag{10}$$

Waveform of exciting impulse function (= switching function) is shown in Figure 2 for 6- and 12-pulses voltages

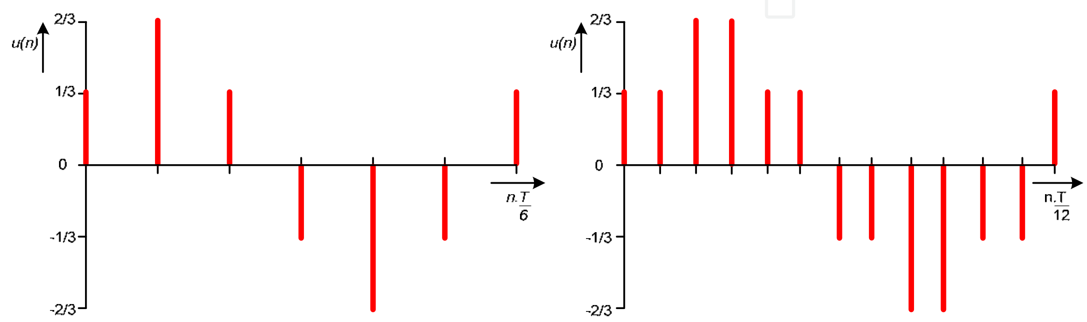

Fig. 2. Switching function of three-phase converter voltage with full width pulses (left)- and PWM modulation 12 pulses (right)

The image of α-component of 6-pulse voltage in z-plain is [Dobrucky et al, 2007]

$$U(z) = \frac{U}{3} \cdot \frac{z^3 + z^2 + z}{z^3 + 1} = \frac{U}{3} \cdot \frac{z \cdot (z+1)}{z^2 - z + 1} \tag{11}$$

Then, the image of α-component of output current in z-plain is

$$I(z) = \frac{U}{3} \cdot \mathrm{g}_{\mathrm{T}/6} \cdot \frac{z \cdot (z+1)}{(z - \mathrm{f}_{\mathrm{T}/6}) \cdot (z^2 - z + 1)} \tag{12}$$

Using inverse z-transform the discrete current series in time-domain will be obtained [Moravcik, 1992].

System decomposition into single harmonic linearised subsystems. Method of investigation assumes decomposition of real electric circuit into ν-harmonic separated equivalent schemes for each harmonic component [Dumitrescu, 2009]; [Benova, 2007]. Then transient analysis can be done for each scheme separately using 'impedance harmonic matrices', and each equivalent scheme is now linearised and therefore easily calculated. After finishing of calculation of each harmonic scheme, the effects of each investigated schemes are summed into resulting quantities of real non-linear electric circuit. That means that cumulative effect of sum of v-harmonic circuits is superimposed on basic harmonic waveform with voltage source.

The equivalent scheme for calculation of state quantities of the network with one appliance is drawn in Figure 3.

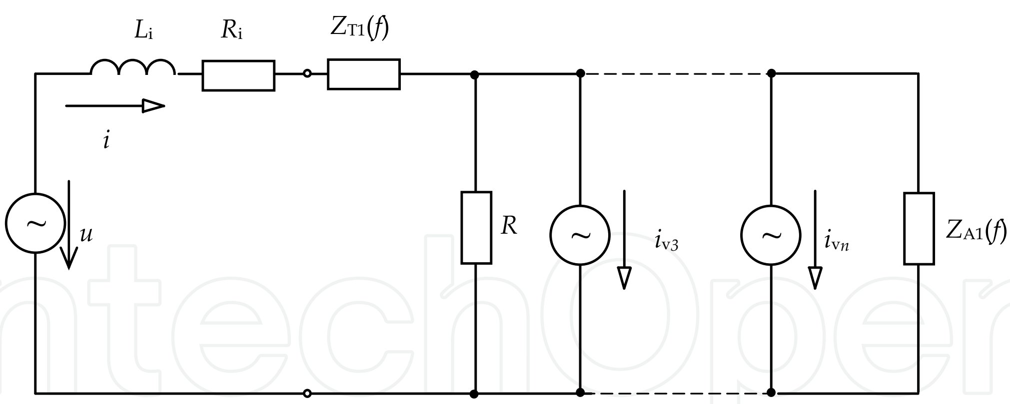

Fig. 3. Equivalent scheme for calculation and state quantities of the network with one R-L appliance for all harmonic components, where $Z_{T1}(f)$ = f(νf_1) and Z_{A1}(f) = f(νf_1) =R_1+j$\nu 2\pi f L_1$, f_1 is frequency of fundamental harmonic component, i_v are current sources representing nonlinearity of appliance, $R = \sum R_v$ is the sum of source resistances

This overall scheme is now decomposed into ν-separate schemes for each harmonic component. These schemes for fundamental- and ν- harmonic components of complex magnitudes will be as in Figure 4a and 4b:

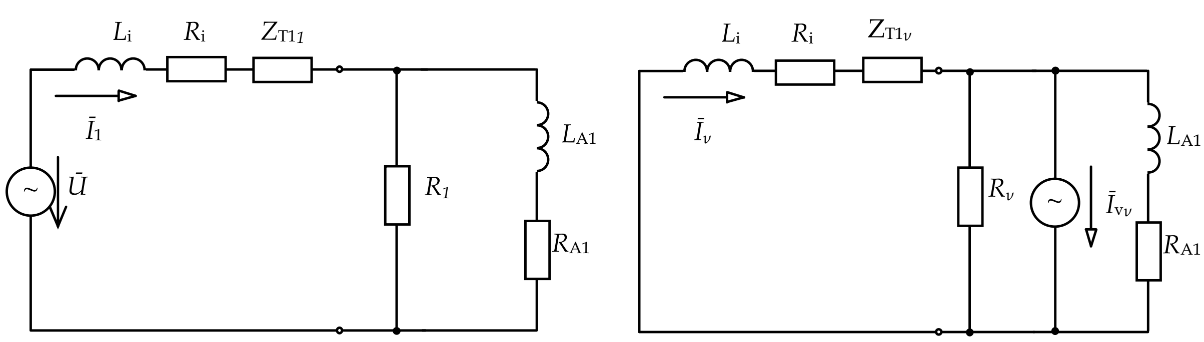

Fig. 4. a,b Equivalent scheme for fundamental (a) and ν - harmonic (b) components of one appliance, where $\bar{U}$ is complex magnitude of network voltage source with voltage of fundamental current source representing nonlinearity of appliance, $\bar{I}_1$ and $\bar{I}_v$ are complex magnitudes of network current for fundamental and ν- harmonic component, $\bar{I}_{vv}$ is complex magnitude of current source representing nonlinearity of appliance

Complex magnitudes of ν-harmonic component can be obtained by harmonic analysis of its current using 'impedance (admittance) harmonic matrices' by nodal voltages for rated power of the appliance. For example, in case of v - harmonic component of one appliance (equivalent scheme on Figure 3b) will be

$$\left(\frac{1}{\overline{Z}_{T1\upsilon}+R_i+\mathrm{j}\nu 2\pi f L_i}+\frac{1}{R_\nu}+\frac{1}{R_{A1}+\mathrm{j}\nu 2\pi f L_{A1}}\right)\cdot\left(\overline{U}_\nu\right)=\left(\overline{I}_{\mathrm{v}\nu}\right) \qquad (13)$$

where $\bar{U}_\nu$ is nodal voltage (equal to appliance voltage in this case). Complex magnitude of network current for ν- harmonic component can be obtained using

$$\bar{I}_{\nu} = \frac{\bar{U}_{\nu}}{\bar{Z}_{T1\nu} + R_i + j\nu 2\pi f L_i} \tag{14}$$

It is possible (after above decomposition) to calculate state quantities of each ν-harmonic.

This overall scheme is now decomposed into ν-separate schemes for each harmonic component. Corresponding harmonic quantities from each scheme are synthesized (summarized) into final resulting waveform of investigated state quantity:

$$i_{total}(t) = i_1(t) + \ldots\ldots + i_n(t) = \Sigma\, i_n(t) \tag{15}$$

After synthesis of all harmonic components the total transient current is obtained.

3. Renewables and non-linear and linear passive and active loads

3.1 Harmonic output voltage RES with non-linear load during transients (island operation)

Single-phase bridge rectifier supplied by stiff voltage (from network or RES with small inner impedance) has positive half-vawes on its DC side as depicted in Figure 5.

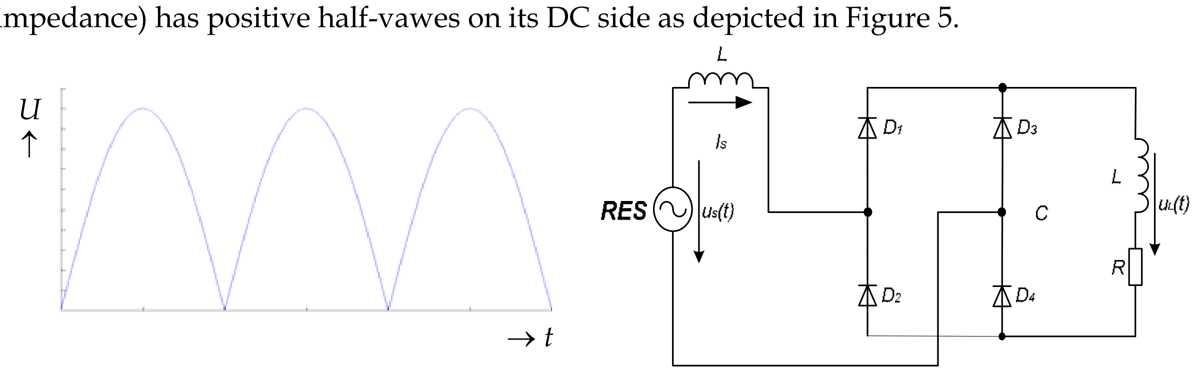

Fig. 5. Scheme of single-phase RES with rectifying load and its DC side voltage

DC voltage can be decomposed into Fourier series as [Bartsch, 1994]

$$u = \frac{4U_m}{\pi}\left[\frac{1}{2} - \frac{1}{1\cdot 3}\cos(2\omega t) - \frac{1}{3\cdot 5}\cos(4\omega t) - \ldots\right] \tag{16}$$

with DC component of $\frac{2U_m}{\pi}$. Supposing R-L load the corresponding current for single harmonic component can be calculated:.

$$i_\nu = \frac{U_\nu}{\left|\bar{Z}_\nu\right|}\left[\cos(\nu\omega t - \varphi_\nu)\right], \tag{17}$$

where

$$\left|\bar{Z}_\nu\right| = \sqrt{R^2 + (\nu\omega L)^2} \tag{18}$$

$$\varphi_\nu = \arctan\frac{\nu\,\omega L}{R} \tag{19}$$

Using synthesis of all harmonic components the total transient current is obtained

$$i_\nu = \frac{U_\nu}{\left|\overline{Z}_\nu\right|}\left[\cos(\nu\omega t - \varphi_\nu) - \cos\varphi_\nu \cdot e^{t/\tau}\right] \tag{20}$$

where $\tau = L / R$.

Note (nota bene): similarly for three-phase 6- pulse middle point rectifier

$$u = \frac{3\sqrt{3}\cdot U_m}{\pi}\left[\frac{1}{2} - \frac{1}{2\cdot 4}\cos(3\omega t) - \frac{1}{5\cdot 7}\cos(6\omega t) - \ldots\right] \tag{21}$$

with DC component of $\frac{3\sqrt{3}\,U_m}{2\pi}$, and also for other types of rectifiers.

Simulation results are given in Figure 6 and Figure 7 for transient and steady-state considering 999 harmonics.

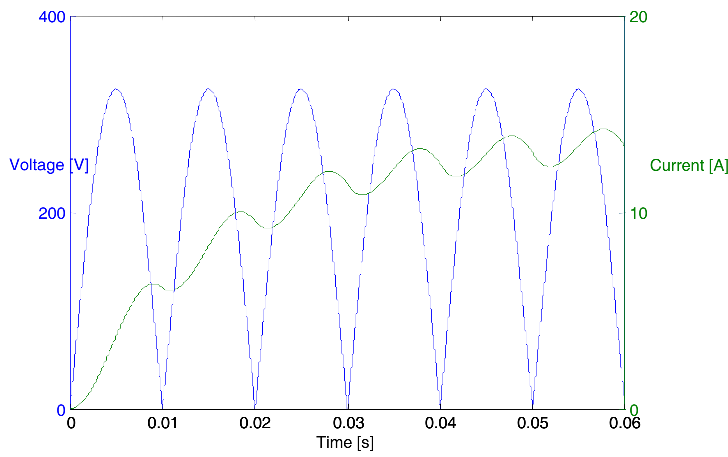

Fig. 6. Dynamic state of connecting nonlinear rectifying load to RES: voltage on DC side (blue) and DC current (green)

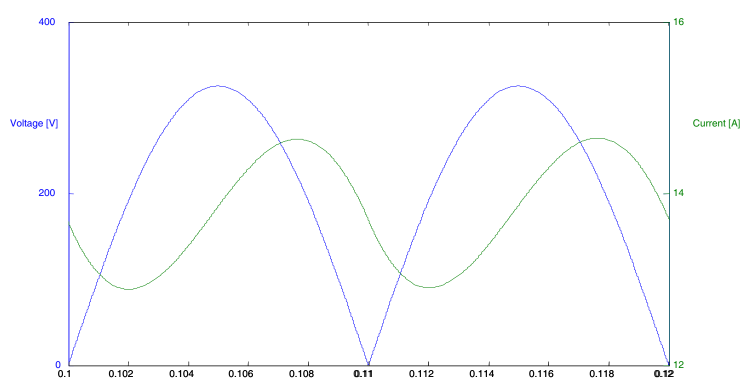

Fig. 7. Steady-state time-vaweforms of DC voltage (blue) and current (green)

3.2 Non-Harmonic output voltage RES with *R-L* load and active voltage source (parallel operation)

Today's converters provide very good quality output quantities regarding to their average and RMS values. Anyway, the output voltage is non-harmonic, switched by high frequency, Figure 8.

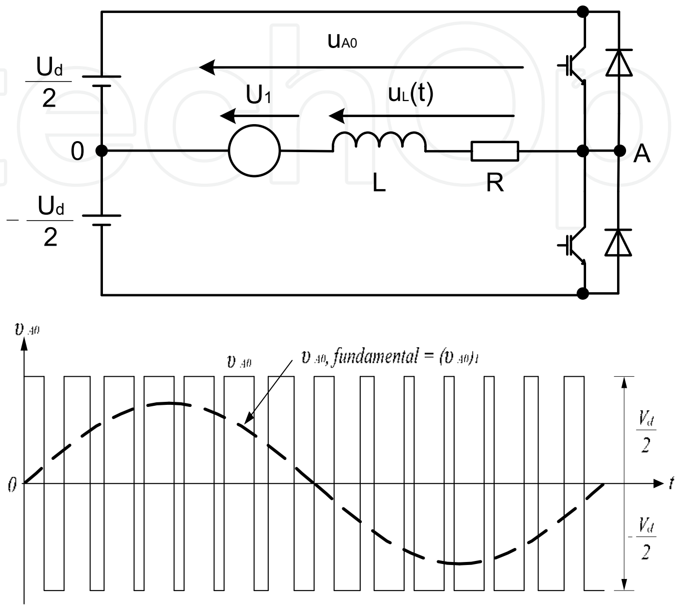

Fig. 8. Scheme of single-phase converter in half-bridge connection (top), and its output voltage

Simulation results for generating and regenerating regimes show Figure 9.

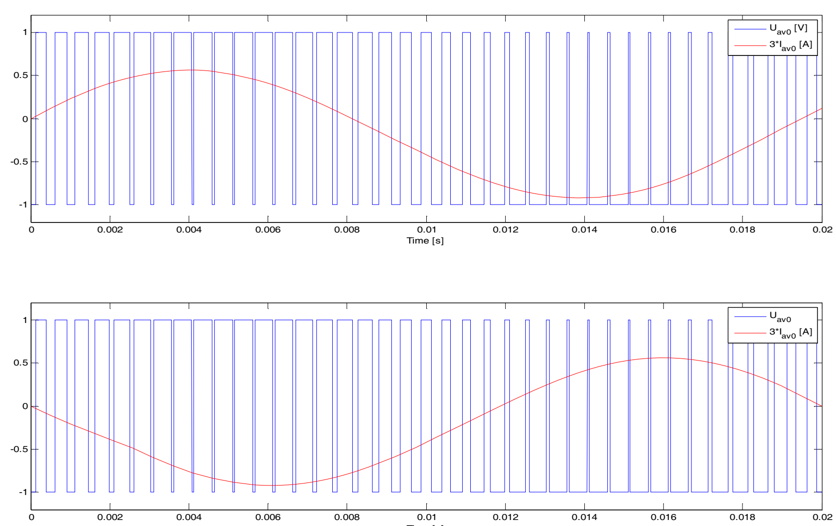

Fig. 9. Time-waveforms of output voltage (blue) and current (red) for generating and regenerating regimes (considering 999 harmonics)

3.3 Three-phase non-harmonic output voltage RES with *R-L* load – behaviour prediction

Three-phase 6-pulse inverter switching function is given in Figure 10.

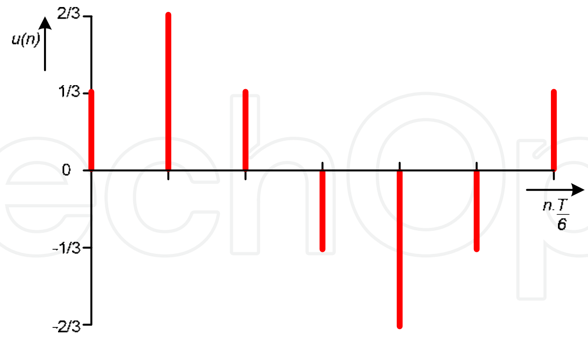

Fig. 10. Switching function for three-phase 6-pulse RES inverter

Corresponding simulation results for complex and time domain are depicted in Figure 11.

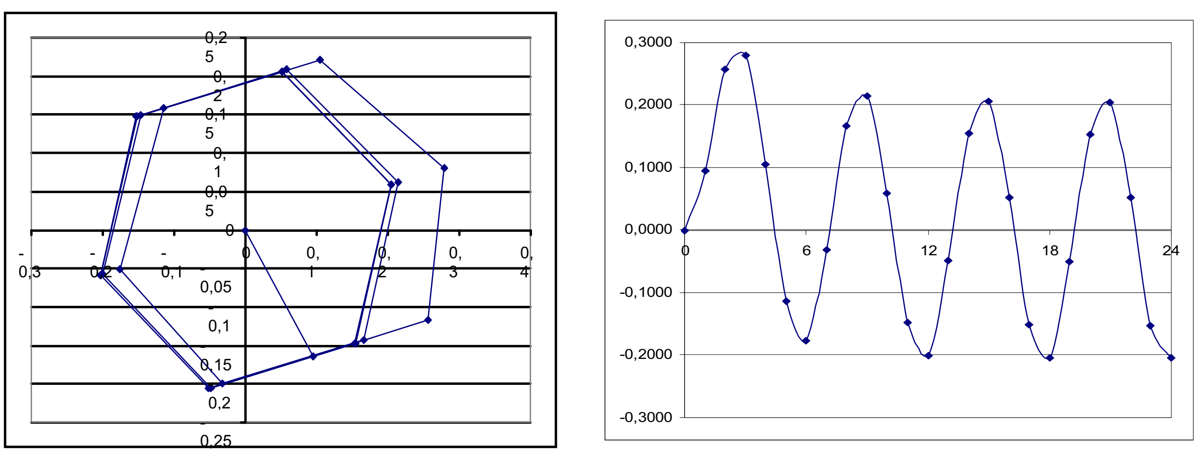

Fig. 11. Trajectories of output voltage in complex (left) and time domain (right)

3.4 Single-phase non-harmonic output voltage RES with *R-L* load – behaviour prediction

Single-phase 2-pulse inverter switching function is given in Figure 12.

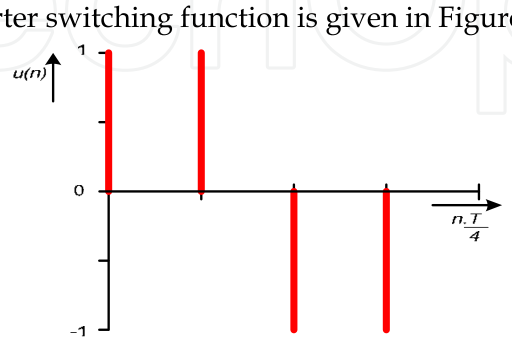

Fig. 12. Switching function for single-phase 2-pulse RES inverter

Corresponding simulation results for complex and time domain are depicted in Figure 13.

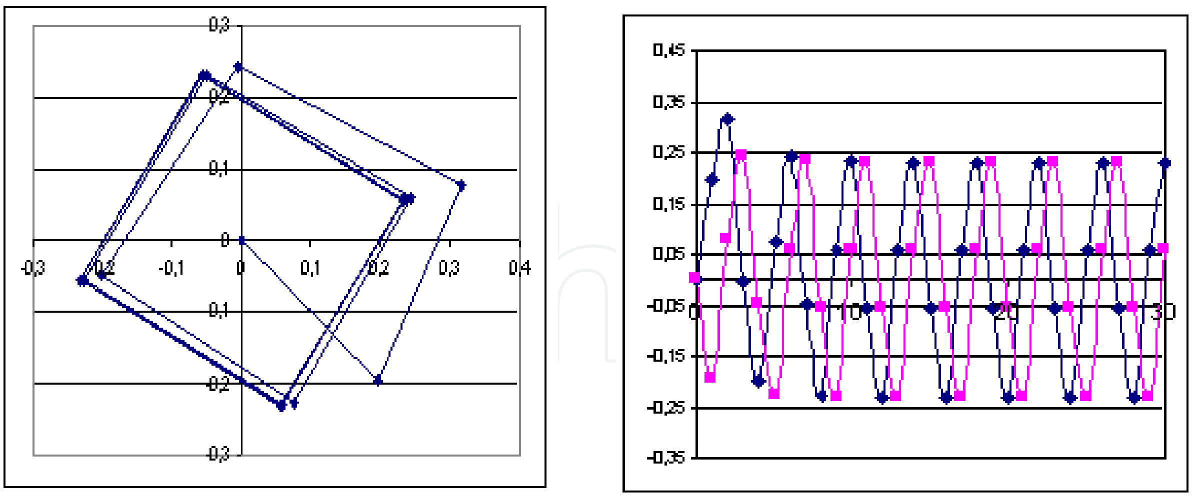

Fig. 13. Trajectories of output voltage in complex (left) and time domain (right)

4. Example of a practical implementation of the introduced methods of solution for different types of operation of RES and power network

The main task of RES system is to deliver power of different composition into power supply network:

- active power delivery (as a priority mission),
- and reactive or/and distortion powers delivery.

Later possibility means that RES provides function of static compensator or/and power active filter. It depends on requests of power supply network what kind of power will be delivered by RES.

The block schemes of connection of both sources and basic scheme of circuit configuration of single-phase voltage inverter are shown in Figure 14.

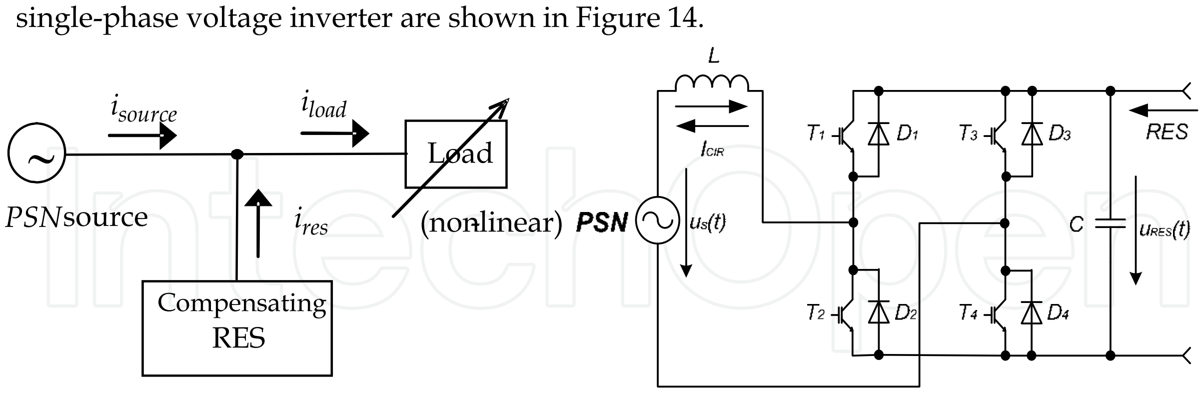

Fig. 14. Basic connection of RES and power network, and circuit configuration of single-phase voltage inverter

Simulation experiments have been carried out by MatLab simulation SW 2008b environment using theory of power active filters [Singh et al, 1999; Dobrucky et al, 2006; Pavlanin et al, 2008] and approach in subsection 3.2 above. Figure 15 shows simulation experiments of active compensation regime depending of time-instant of full load switching-on.

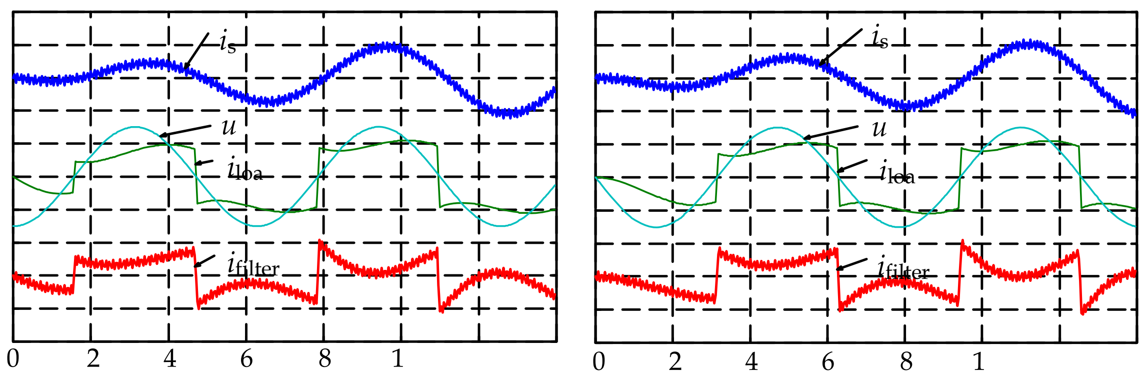

Fig. 15. Simulation of RES in active compensation regime: Load switched-on at negative maximum of voltage (left) and in optimal instant of time (right)

During compensation regime of RES the complementary compensating current i_{res} is generated by such a way, that after its addition with non- sinusoidal and phase shifted load current i_{load}, the only active power (e.g. active and harmonic current i_{source}) will be delivered by supplying network:

$$i_{load} = i_{res} + i_{source} \tag{22}$$

The calculation of this compensating current is the most important activity of the active filter's control circuit. The calculations can be carried out by different ways [Singh et al, 1999; Dobrucky et al, 2006; Pavlanin et al, 2008].

Simulation of RES in regime delivering of active power can be observed in subsection 3.2. Active power can be delivered to- or taken from power supply network.

5. The results of laboratory experiments

There are oscilloscopic records from experimental verification of RES operation in Figs. 16, 17, 18, 19 and Figure 20 for both compensation and active power delivering.

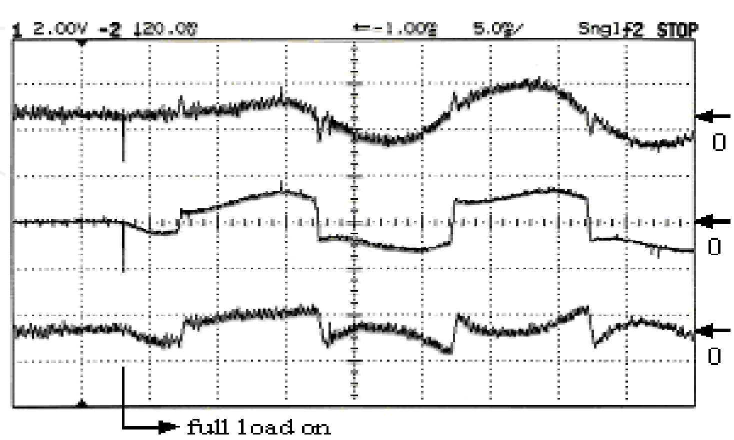

Fig. 16. Transient response of RES for the full load switched on: source current (top), load current (middle) and RES current (bottom) [Dobrucky et al, 2006]

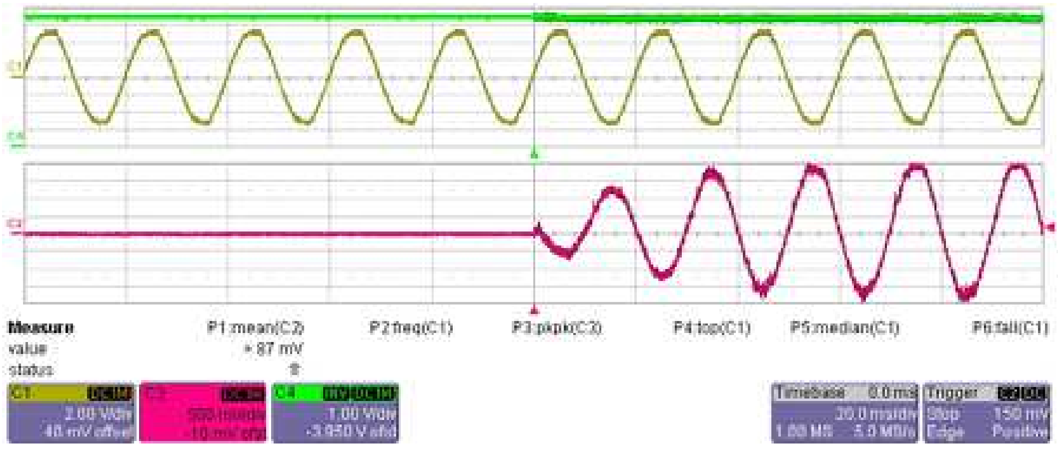

Fig. 17. Switching-on of the RES delivering pure active current [bottom, red] into power supply network (top, yellow)

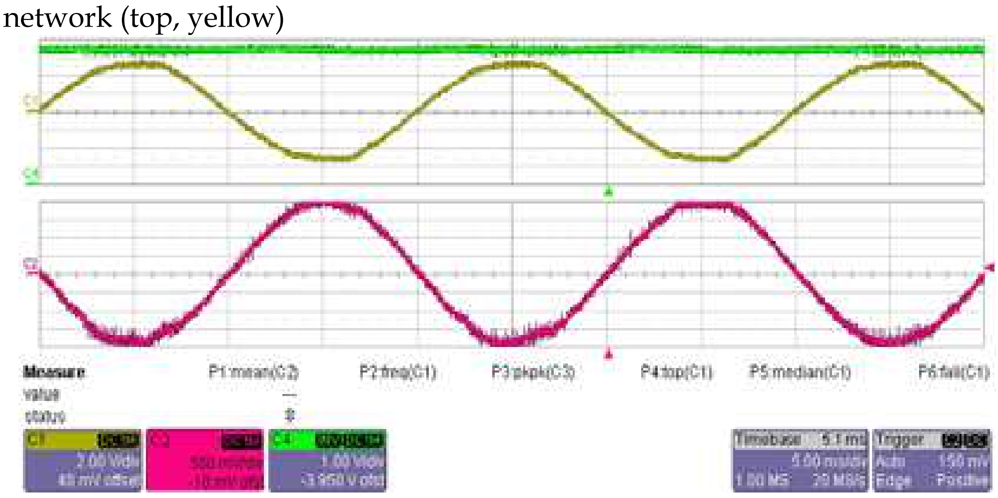

Fig. 18. Steady-state operation of RES in regime of active power delivering: voltage (top) and current (bellow)

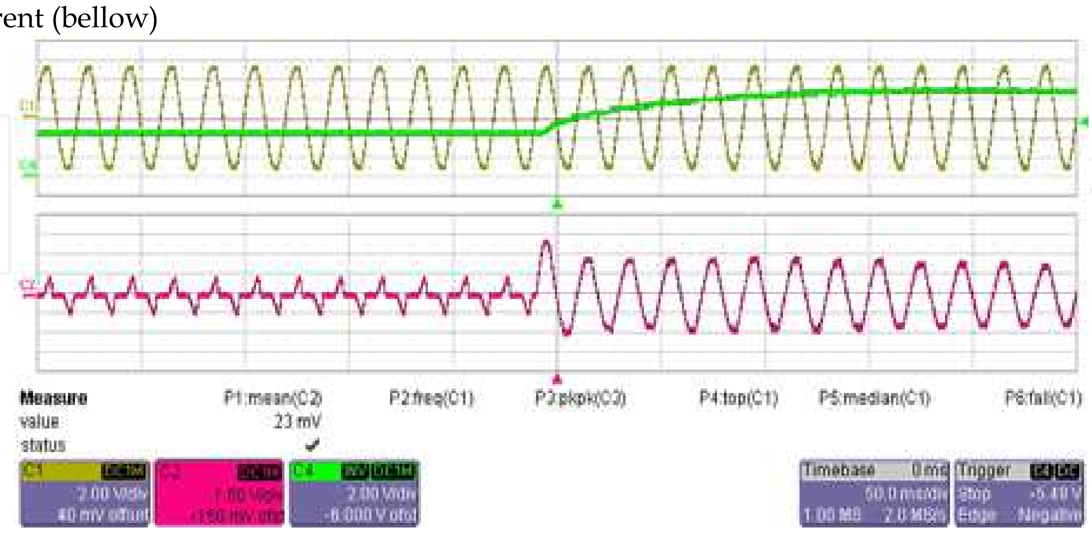

Fig. 19. Transient record of RES in regime of power acceptor from network: network voltage (top, yellow), voltage of DC bus (top, green) of RES and current (bellow)

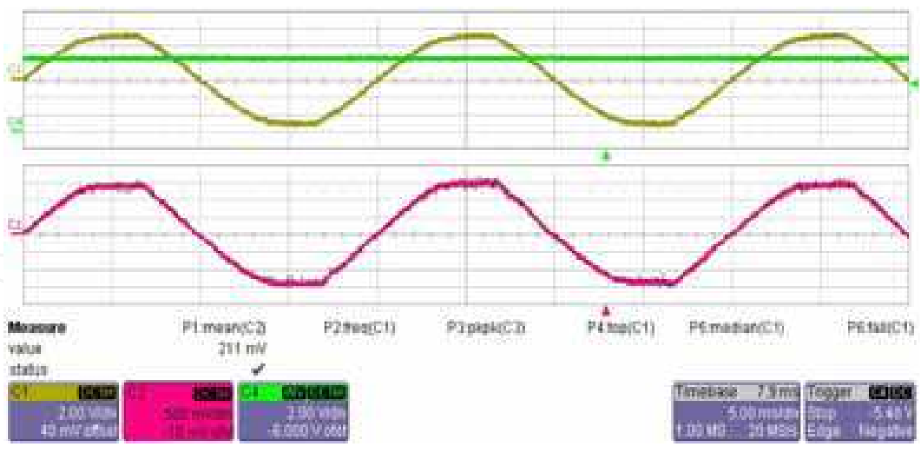

Fig. 20. Steady-state operation of RES in regime of power acceptor from network: voltage (top) and current (bellow)

6. Evaluation and conclusion

It has been shown that renewable energy source can work in two regimes of operation: as power generating or power consumption unit. Simulation and experimental results have proved **excellent transient properties** of the RES in both operations. As can be seen in Figure 16 and 17, respectively, the waveforms indicate an instantaneous reaction of compensation in generic regimes of RES. RES reacts already after the first calculation step Δt, so it is possible to use it as dynamic voltage restorer for small changes of the supply voltage.

7. References

Bala, S. & Venkataramanan, G. (2007). Balanced Power Aggregation of Asymmetric Single-phase Systems. *IEEE Power Electronics Specialists Conference (PESC'07)*, pp. 2772-2778, ISBN: 978-1-4244-0655-5, Orlando, FL, USA, June 2007

Bartsch, H.J. (1994). *Mathematic Formulae*, 4th revised edition (in German), Carl Hanser Publisher, ISBN 80-200-1448-9, Munich (DE)

Benova, M. (2007): *Non-sinusoidal Current and Voltage Analysis with regard to Power Condition of Electrical Machines* (in Slovak), PhD thesis, Faculty of EE, University of Zilina (SK), pp. 115

Burger, B. & Engler, A. (2001). Fast signal conditioning in single phase systems, *9th European Conference on Power Electronics and Applications*, pp. CD-ROM, ISBN, conference Graz (AT),1991

Dobrucky, B. Drozdy, S., Frivaldsky, M. & Spanik P. (2007). Interaction of Renewable Energy Source and Power Supply Network in Transient State, *Proc. of ICCEP'07 Int'l Conf. on Clean Energy Power,* pp. CD-ROM, *Capri* (IT), May 2007

Dobrucky, B., Marcokova, M., Pokorny, M. & Sul, R. (2007). Prediction Of Periodical Variable Structure System Behaviour Using Minimum Data Acquisition Time, *Proc. of IASTED MIC'07 Int'l Conf. on Modelling, Identification, and Control*, pp. CD-ROM, , Innsbruck (AT), Feb. 2007

Dobrucky, B. & Pokorny, M. (2006). Highest Dynamics and Ultra Fast Start-Up of Power Active Filter. *International Review of Electrical Engineering*, No. 8, Aug. 2006, pp. 391-399, ISSN 1827-6660

Dumitrescu, M.: Harmonic Digital Simulation Technique on an Industrial Environment. Electrical Review (Przeglad elektrotechniczny, PL), No. 1 (85), 2009, pp. 217-221, ISSN 0033-2097

Ghartemani, M. K., H. Mokhtari, M. R. Iravani, A Signal Processing System for Extraction of Harmonics and Reactive Current of Single-Phase Systems, *IEEE Trans. on Power Delivery, Vol. 19*, July 2004, pp. 979-986

IEEE, (1999). *Standard 519-1992 Power Grids Distortion Limits. Voltage characteristics of electricity supplied by public distribution systems*, European Norm EN 50160

IEEE (2000). *Trial-Use Standard Definitions for the Measurement of Electric Power Quan-tities Under Sinusoidal, Nonsinusoidal, Balanced, or Unbalanced Conditions*. IEEE Standard 1459

Koutroulis, E., K. Kalaitzakis, N.C. Voulgaris: Development of a Microcontroller-Based Photovoltaic Maximum power Point Tracking Control System. *IEEE Trans, on Power Electronics*, Vol. 16, No. 1, Jan. 2001, pp. 46-54

Marcokova, M. & Guldan V. (2009). On one orthogonal transform applied on a system of orthogonal polynomials in two variables. *Journal of Applied Mathematics*, Vol. 2, No. 2, pp. 239 - 245

Marcokova, M. (1995): Equiconvergence of Two Fourier Series. Journal of Approximation Theory, Vol. 80, No. 2, , pp. 151-16

Mohan, N., Undeland, T.M. & Robbins, W.P. (2003). *Power Electronics : Converters, Applications, and Design 3rd Edition*, John Wiley & Sons, Inc., ISBN 0-471-42908-2, New York

Pavlanin, R. & Spanik, P. (2008). Effect of PCC Voltage Distortion on Shunt active Power filter Function (in Slovak), *Proc. of 8th ERU08 Conference, on Electromagnetic Disturbation in Distributed- and Industrial Networks*, pp. CD-ROM, ISBN 978-80-254-3821-3, Brno (CZ), Nov. 2008

Rajeshekara, K. (2005). Hybrid Fuel-Cell Strategies for Clean Power Generation. *IEEE Trans, on Industry Application*, Vol. 41, No. 3, May-June 2005, pp. 682-689,

Singh, B., Al-Haddad, K., & Chandra, A. (1999). A review of active filters for power quality improvement. *IEEE Transactions on Industrial Electronics*, Vol. 46, pp. 960–971, Oct. 1999

Takeuchi, T.J. (1973). *Theory of SCR Circuit and Application to Motor Control*. Electrical Engineering College Press, 1968 - Russian Edition, Energia Publisher, Leningrad-St. Petersburg (RF), 248 pp., T 051(01)-73 130-73, Tokyo (JP)

CIGRE Working Group (2007). *C4.601 Modeling and Dynamic Behavior of Wind Generation Relates to Power System Control and Dynamic Performance,* CIGRE, August 2007,

Xue, Y., Chang, L., Kjaer, S. B., Bordonau, J. & Shimizu, T. (2004). Topologies of Single-phase Inverters for Small Distributed Power Generators: An Overview. *IEEE Transactions on Power Electronics*, Vol. 19, Sept. 2004, pp. 1305– 1314

Zaskalicky, P. & Zaskalicka M. (2009). Complex Fourier Series Model of a Three-Phase Voltage Source Inverter, *Acta Electrotechnica et Informatica*, Vol. N, No. X, 2009 (accepted)

Renewable Energy
Edited by T J Hammons

ISBN 978-953-7619-52-7
Hard cover, 580 pages
Publisher InTech
Published online 01, December, 2009
Published in print edition December, 2009

InTech Europe
University Campus STeP Ri
Slavka Krautzeka 83/A
51000 Rijeka, Croatia
Phone: +385 (51) 770 447
Fax: +385 (51) 686 166
www.intechopen.com

InTech China
Unit 405, Office Block, Hotel Equatorial Shanghai
No.65, Yan An Road (West), Shanghai, 200040, China
中国上海市延安西路65号上海国际贵都大饭店办公楼405单元
Phone: +86-21-62489820
Fax: +86-21-62489821